Published in Computational Materials Science 33(1-3): 175-183, 2005

FP-LAPW investigation of electronic structure of TaN and TaC compounds

M. Sahnoun [a,b,*], C. Daul [a], M. Driz [b], J.C. Parlebas [c], C. Demangeat [c]

[a] *Department of Chemistry, University of Fribourg, Chemin du Musée 09, Fribourg CH-1700, Switzerland*
[b] *Laboratoire de Physique Quantique et de Modélisation Mathématique (LPQ3M), Département de Technologie, Université de Mascara, DZ-29000 Algeria*
[c] *IPCMS-GEMM, UMR 7504 CNRS, 23 Rue du Loess, F-67034 Strasbourg Cedex 2, France*

Abstract

We study the structural and electronic properties of tantalum compounds, i.e. TaC and TaN, by means of accurate first principle total energy calculations using the full-potential linearized augmented plane wave plus local orbitals (FP-LAPW + *lo*) method. The calculations are based on density functional theory and we use the local density approximation (LDA) as well as the generalized gradient approximation (GGA) for the exchange and correlation potential. The calculated electronic structure, total energies, and equilibrium lattice constants are determined for the NaCl structure of TaC and TaN, and these results are discussed in terms of the nature of bonding found in these compounds. In both tantalum compounds studied the Ta 5d-like and N(C) 2p-like states are strongly hybridized. The values of the lattice constants, bulk moduli, and elastic constants have been calculated and are in reasonable agreement with experiment and other theoretical works.

PACS: 71.20; 71.20.B; 71.15.M; 62.20.D
Keywords: FP-LAPW + *lo*; Elastic constants; Electronic band structure; Transition metals

1. Introduction

Transition metals form binary carbides and nitrides, which have been considerably investigated because of their unique chemical and physical properties, such as high melting point, chemical inertness, superior hardness, and metallic electrical conductivity [1–7]. The phase diagrams of the

* Corresponding author. Address: Department of Chemistry, University of Fribourg, Chemin du Musée 09, Fribourg CH-1700, Switzerland. Tel.: +41 26 300 87 49; fax: +41 26 300 97 38.
E-mail address: mohammed.sahnoun@unifr.ch (M. Sahnoun).

0927-0256
doi:10.1016/j.commatsci.2004.12.010

binary systems Ta–C and Ta–N display, like that of niobium, a variety of stable carbide and nitride phases [8–11], which are suitable for special mechanical applications [12]. These two systems have gained considerable importance as a diffusion barrier in advanced semiconductor device technologies [13,14]. Several transition metals and their nitrides films, such as Ta, TaN, TiN and WN, have been considered as the most promising candidates for a diffusion barrier in Cu interconnects [14–18]. Recently, TaC and TaN have attracted increasing attention among researchers due to their excellent thermal stability and chemical inertness to copper at elevated temperatures [18–22].

Mechanical properties usually are interpreted and evaluated in terms of microstructure, grain size and influence of the chemical composition. To make things really complicated, the texture, grain size, crystallite size and defects, in general, also depend on the composition and process parameters. It appears of prime importance to reconsider the fundamental relationships between the occupancy of the valence electronic states and the physical properties by considering the crystalline structure. By the inclusion of this aspect, the aim of the present research is to establish a general basis allowing the interpretation and the prediction of the physical properties, as a function of distinctive features of the electronic band structure.

In this paper we present the results of studies of the electronic structure of stoichiometric TaC and TaN. The calculations have been done using the full-potential linearized augmented plane waves plus local-orbital method (FP-LAPW + *lo*) [23–25] based on density functional theory.

2. Calculation method

In this work, the states treated as bands were: Ta(5s, 5p, 5d, 6s), N(2s, 2p) and C(2s, 2p). We note that the Ta 4f states which lie in the lower valence-band region were treated as core states due to their extremely small k-space dispersion. The lattice is divided into muffin-tin spheres and interstitial region; the muffin-tin radii chosen are 2.0, 1.8, and 1.8 a.u. for Ta, N, and C, respectively. Inside the muffin-tins, the basis functions are expanded into spherical harmonics up to order $l = 10$. In the interstitial region the basis functions are expanded into plane waves. In addition, the electron–electron exchange interaction is described using the generalized gradient approximation (GGA) as well as the local density approximation (LDA). The GGA employed a Perdew–Burke–Ernzerhof (PBE96) functional form [26], and a Ceperley–Alder [27] form is employed for the correlation part in LDA.

Extended test calculations have proven to yield sufficient accuracy in total energy minimization of bulk TaC and TaN using only 72 k-points inside the irreducible wedge of the Brillouin zone, an energy cut-off of the plane wave expansions in the interstitial region of $RK_{max} = 8$, and $l_{max} = 10$ for the upper limit of the angular momentum expansions of the wave functions inside the nonoverlapping spheres surrounding the atomic sites. The radial basis functions within the muffin-tin spheres are linear combinations of radial wave functions and their energy derivatives were computed at energies appropriate to their site. Outside the muffin-tin spheres the basis functions are plane waves expanded in a Fourier series. All results represented here are obtained with a convergence criterion of 0.1 mRy for the energy eigenvalues. The ab initio calculation of the valence and conduction band energy eigenvalues has been performed at 111 points including five high symmetry points W, L, Γ, X and K.

The elastic moduli of a cubic crystal may be divided into two classes, the bulk modulus $B = (C_{11} + 2C_{12})/3$, and the two shear moduli, $C_{11} - C_{12}$ and C_{44}. The bulk modulus is related to the curvature of $E(V)$,

$$B(V) = -VP'(V) = VE''(V) \tag{1}$$

where V is the volume of the unit cell, $E(V)$ is the energy/unit cell at volume V, and $P(V) = -E'(V)$ is the pressure required to keep the cell at volume V. The calculations only provide a set of energies $E(V_i)$ for a finite number of volumes V_i and the second derivative $E''(V)$ has to be approximated. In order to estimate $E''(V)$ we perform a least squares fit of the computed energies to the model proposed by Murnaghan [28]:

$$E = \frac{BV}{B'}\left(\frac{1}{B'-1}\left(\frac{V_0}{V}\right)^{B'} + 1\right) + E_0 \tag{2}$$

where E_0, V_0, B, and B' are, respectively, the equilibrium energy, volume, bulk modulus, and its pressure derivative. The bulk modulus can then be obtained by analytic differentiation of Eq. (2), $B = V\partial^2 E/\partial V^2$.

The shear moduli require knowledge of the derivative of the energy as a function of lattice strain [29]. In the case of a cubic lattice, it is possible to choose this strain so that the volume of the unit cell is preserved and the energy is an even function of the strain. Hence an expansion of the energy into a power series of the strain contains no odd powers. Thus for the calculation of the modulus $C_{11} - C_{12}$ we use the volume-conserving orthorhombic strain tensor,

$$\bar{\varepsilon} = \begin{pmatrix} \varepsilon & 0 & 0 \\ 0 & -\varepsilon & 0 \\ 0 & 0 & \varepsilon^2/(1-\varepsilon^2) \end{pmatrix} \tag{3}$$

Application of this strain changes the total energy from its unstrained value to

$$\begin{aligned} E(\varepsilon) &= E(-\varepsilon) \\ &= E(0) + (C_{11} - C_{12})V\varepsilon^2 + \mathrm{O}[\varepsilon^4] \end{aligned} \tag{4}$$

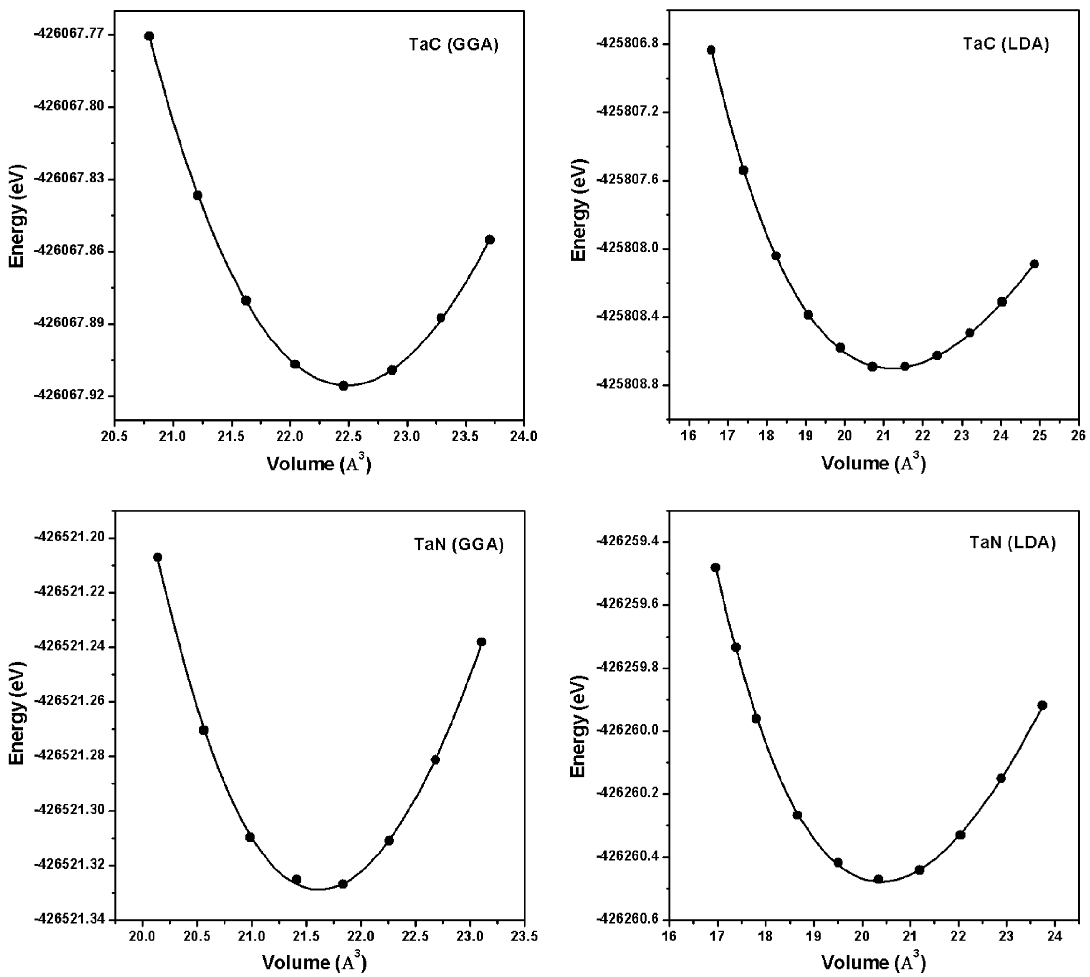

Fig. 1. Energy versus volume curves of the rock-salt TaC and TaN, calculated in LDA and GGA approximations.

where V is the volume of the unit cell and $E(0)$ is the energy of the unstrained lattice at volume V.

For the elastic modulus C_{44}, we use the volume-conserving monoclinic strain tensor

$$\bar{\varepsilon} = \begin{pmatrix} 0 & \varepsilon/2 & 0 \\ \varepsilon/2 & 0 & 0 \\ 0 & 0 & \varepsilon^2/(4-\varepsilon^2) \end{pmatrix} \tag{5}$$

which changes the total energy to

$$E(\varepsilon) = E(-\varepsilon) = E(0) + \frac{1}{2}C_{44}V\varepsilon^2 + \mathrm{O}[\varepsilon^4] \tag{6}$$

3. Results and discussions

3.1. Structural and elastic properties

In this study, two different exchange-correlation potential functions, the LDA and GGA, where employed to characterize the atomic behavior of TaC and TaN. In many cases, the two potential functions provide comparable results (i.e., Fig. 1). In this study, as a matter of convenience only, the LDA results are presented in all figures. Furthermore, as mentioned, in Table 1 all the LDA and GGA results are presented for each parameter.

In Table 1, we give our calculated values of the equilibrium lattice constants, bulk modulus, and its pressure derivative for TaC and TaN, as well as the experimental and other theoretical values. We notice from this table that our LDA results for the equilibrium lattice constants are slightly smaller by 1.3% compared to the experimental values for both TaC and TaN. However, when we use the GGA these calculated lattice constants are slightly larger by 0.7% of the experimental values for both TaC and TaN. For the calculated values of the bulk modulus (B), we notice that the value given by the LDA for TaC is overestimated with regards to the experimental value by 16%, whereas the GGA result is underestimated by 7%. For TaN, the calculated value of B in the LDA is larger than the experimental value about 18.4%, while the GGA value is underestimated by 3.7%.

Our calculated elastic constants are listed in Table 1. For TaC we see that the calculated values of C_{11}, C_{12} and C_{44} in the LDA are larger than the experimental values. When we use GGA, these calculated values of C_{11} and C_{44} are underestimated, but C_{12} is overestimated in comparison with the experimental data. No experimental data are available for TaN, but our calculated values of C_{11}, C_{12} and C_{44} are in reasonable relation to those of TaC. We can consider the present study of elastic constants as a good prediction of the experimental observations.

Table 1
Calculated and experimental lattice constant a_0, bulk modulus B, their energy derivative B', and elastic constants of TaC and TaN

		TaC				TaN			
		LDA	GGA	Theo.	Exp.	LDA	GGA	Theo.	Exp.
a_0	(Å)	4.39	4.48	4.46[a]	4.46[b], 4.45[c]	4.33	4.42	4.42[a], 4.39[d]	4.427[e]
B_0	(GPa)	397.6	318.98	342[a]	317[f]	403.85	328.3	341[a]	
B'		3.64	4.34	–	–	4.28	5.45	–	–
C_{11}	(GPa)	880.37	732.86	–	500[g], 550[g]	886.90	675.95	–	
C_{12}	(GPa)	156.24	112.04	–	90[g], 150[g]	162.33	154.48	–	
C_{44}	(GPa)	410.44	315.47	–	80[g], 190[g]	355.86	266.92	–	

[a] Ref. [30].
[b] Ref. [3].
[c] Refs. [31,32].
[d] Ref. [33].
[e] Ref. [34].
[f] Ref. [35].
[g] Ref. [36].

3.2. Electronic structure and chemical bonding

In Figs. 2 and 3 the DOS's and the energy bands corresponding to the B1 structure of TaC and TaN are shown. The overall features are similar to those of previously published [32,37–49] carbides and nitrides. In Table 2 the values of characteristic band separations are even. We select for comparison the gap E_g between the C(N) s band and the valence-band complex, the zone-center d-band splitting $\Delta E_d \equiv E(\Gamma_{12}) - E(\Gamma_{25'})$, the Ta d–C(N) p splitting $E_d - E_p$ [$E_d \equiv \frac{2}{5}E(\Gamma_{12}) + \frac{3}{5}E(\Gamma_{25'})$ and $E_p \equiv E(\Gamma_{15})$]. We also select other energy differences e.g.

$E(\Gamma_{15}) - E(L_1)$: width of the 2p-bands.

$E_F - E(L_1)$: width of the occupied part of the 2p and 5d-bands in the case of overlap.

$E_F - E(X_3)$: width of the occupied part of the 5d-bands.

The essential features of the band structure found in our calculations are in a good agreement with the results reported by Papaconstantopoulos [37], Gupta and Freeman [44] using the APW method, as well as with many others [40,45].

In comparison, we notice that the Fermi level moves up in energy, since the number of valence electrons increases from eight to nine for TaC and TaN, respectively. Therefore, the increase of E_F is caused by the additional valence electron.

From Table 2, one can clearly see that the width of the nonmetal p-band from L_1 to Γ_{15} is larger for TaN than for TaC, because in these bands, there is a strong mixing of pd_σ with pd_π in TaN. It is interesting to note that the E_g values at L-points (of the order of ≈4.82 eV) for TaN is greater than in TaC (with E_g = 1.1 eV), indicating the increase of the ionicity in TaN in comparison to TaC. However, the quantity $E_d - E_p$ which is a measure of the relative positions of the Ta-d and X-p bands, increases from TaC to TaN, indicating a decrease of the overlap and of the mixing between these two bands. Therefore, we suggest that they provide an adequate description of this phenomenon because the extra electron added in TaN occupies primarily into open d-states. So we can deduce that there is a decrease of covalence in these compounds. Hence, the covalent bonding character is strongest in the carbide and reduced in the nitride.

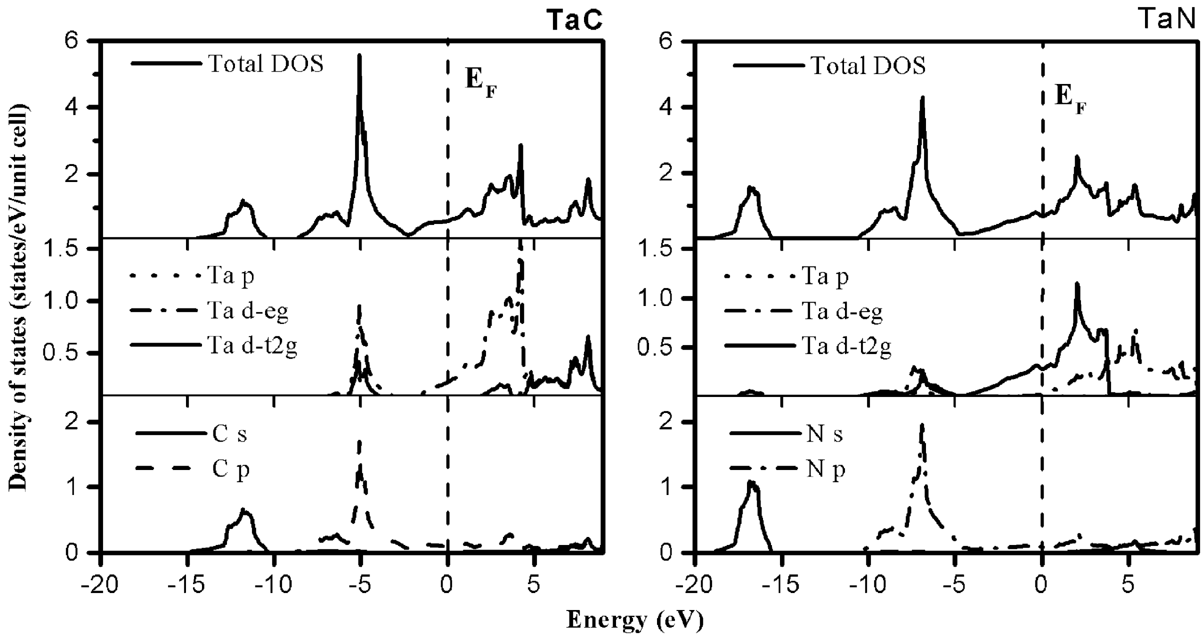

Fig. 2. The density of states (DOS) obtained by the LDA calculation of TaC and TaN (in states per eV unit cell).

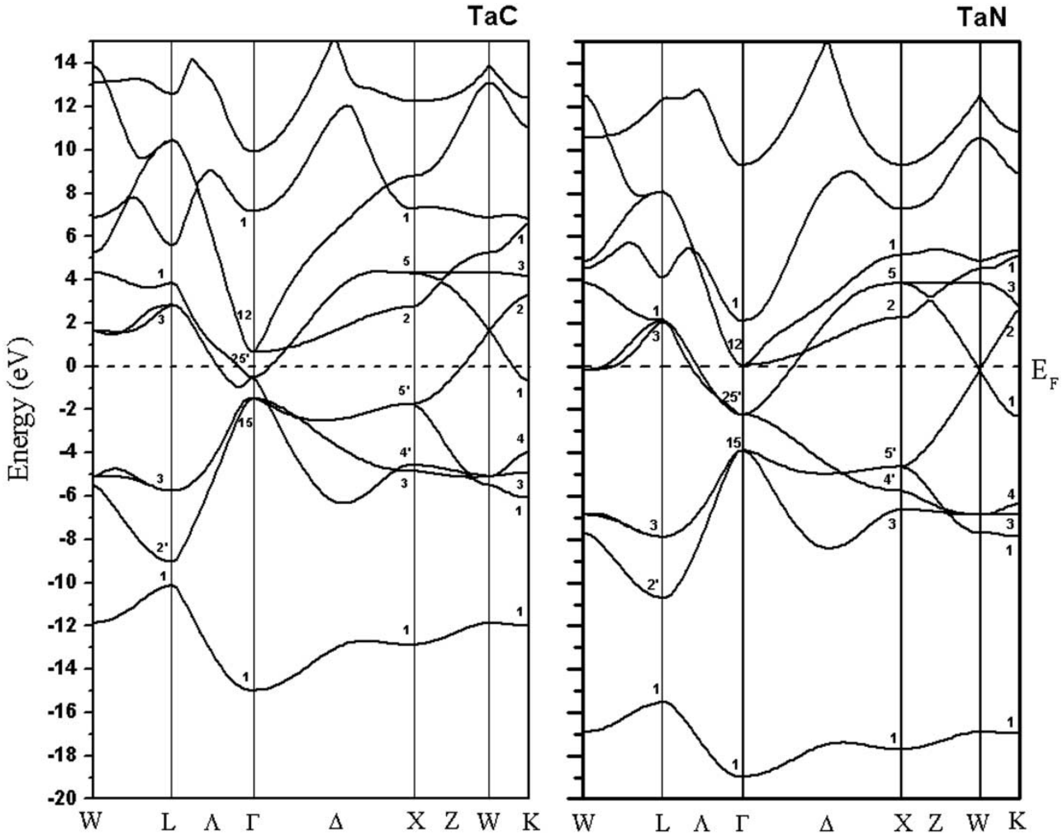

Fig. 3. Electronic energy band structure obtained by the LDA calculation of TaC and TaN.

Table 2
Energy separation (eV) of characteristic bands defined in the text, Fermi-level (eV) and density of states $N(E_F)$ (eV spin unit cell)$^{-1}$ for TaC and TaN

	E_g	ΔE_d	$E_d - E_p$	$E_F - E(X_3)$	$E_F - E(L_1)$	$E(\Gamma_{15}) - E(\Gamma_1)$	E_F	$N(E_F)$
TaC	1.10	1.15	1.44	4.84	9.03	13.49	1.24	0.60
TaN	4.82	2.28	2.55	6.61	10.69	15.11	1.34	0.69

The covalent interactions in these compounds occur mainly between X-p and Ta-d atomic states. It is interesting to note that $E_d - E_F$ for TaC, i.e. about -0.043 eV, is also an indication of the strong hybridization between metal and nonmetal states near E_F. The large p–d interaction mixes the bands so thoroughly that the total and partial DOS's (Fig. 2) appear very similar.

The DOS of the valence-band complex is characterized by two-high-density regions separated by a low-density region (sometimes designated as a bonding-anti-bonding gap). The lower, bonding states are of two types: a metal Ta s–C(N) p combination at the bottom, with a larger metal Ta d–C(N) p bonding combination just above. It is this strong mixing, which places most of the occupied valence states below E_F, that is thought to be related to the strong bonding properties of several related transition-metal carbides and nitrides. The upper region of the valence-band complex, ranging from somewhat below E_F to roughly 3 eV for TaC and 5 eV for TaN above E_F, is primarily composed of metal Ta-d states, but also contains a small C(N)-p component (typically 10–15 at.% E_F) which can influence material properties to some extent (e.g. superconductivity, see Ref. [37,46]).

In Fig. 2 the Ta d DOS is broken down into its e_g and t_{2g} components. This decomposition illustrates that most of the d states which are occupied in TaC and TaN (with $E_F = 1.24$ and 1.34 eV, respectively) are t_{2g} states.

The mean contribution to bond strength is given by covalent interaction between Ta and X (X = C or N) atoms. The covalent bonding is a result of the overlap between X-2p and Ta-d atomic orbitals. The essential conditions for a strong covalent bonding [47] are strong overlaps between participating orbitals, as well as comparable energy sizes of those orbitals. Those conditions are nicely met in TaC [47], and to a similar degree in other carbides and nitrides as well [47,48]. A schematic illustration of the contributing Ta-d and X-2p orbitals and the areas of their overlap are given in Fig. 4.

From general chemical and wave-function-symmetry considerations one can show that the Ta d–e_g orbitals can interact with C (or N) sp orbitals forming σ bonds, and the Ta d–t_{2g} orbitals can form π bonds with C (or N) p electrons. Note that the overlapping of the symmetry adapted combination (see Fig. 4) can form p–d bonding and anti-bonding states, and their occupation with electrons results in a redistribution of the electron charge density in space, which implies some degree of charge transfer between Ta and C(N) atomic spheres. This charge transfer is responsible for the ionic contribution to the Ta–X (X = C, N) bonding, which can be viewed as electrostatic interaction between charged Ta and C(N) atomic spheres. The direction of the electron transfer is typically from metal to nonmetallic atoms. There is a transfer of roughly 1.0 and 0.95 electrons from Ta to C(N), respectively in TaC and TaN.

Using Electron spectroscopic measurements of binding energy shifts in Group 4*b*, 5*b* and 6*b* carbides [49,50], it was found that electrons are transferred from the metal to the carbon atoms when a carbide of this type is formed.

The metallic component of the TaX (X = C, N) cohesion comes from the interaction of the d-orbitals of the neighboring Ta atoms in the Ta sublattice. Similarly to the covalent Ta–C(N) bonding, Ta–Ta bonding is due to the interaction of the overlapping atomic orbitals (Fig. 4(b)). To get a simple insight into the Ta–Ta bonding we start from a picture of metallic d–d bonding in the fcc-Ta. The first step in the formation of Ta–C(N) compound is to expand the fcc-Ta lattice to the size it has in the Ta–C(N) compound. Such

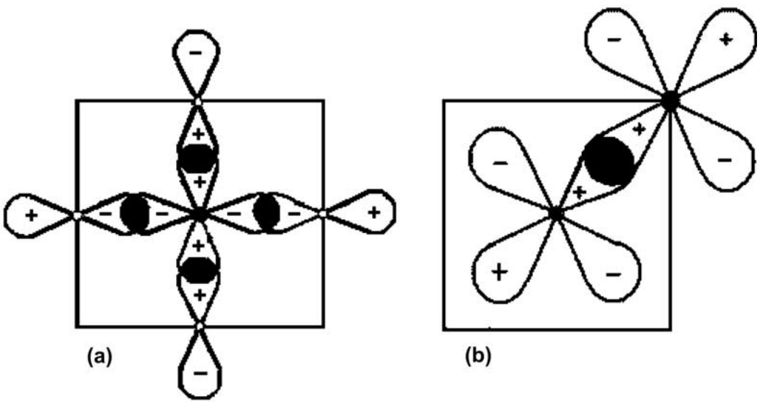

Fig. 4. Schematic illustration of the main overlapping of the metal, Ta, (filled circles) and nonmetal X = C, N, (unfilled circles) atoms in the (001) plane of the NaCl structure: σ-bonding between Ta-d and X-p orbitals; (b) σ-bonding between Ta-d orbitals of the neighboring Ta atoms.

an expansion increases the distances between the nearest Ta neighbors, thus decreasing the overlap between the atomic d-orbitals, and hence leading to a weaker bond. The energy cost of such an expansion is analysed for other transition metals in Ref. [51].

An even more important modification of the Ta–Ta bonding is due to formation of the Ta–C(N) bonding and anti-bonding states. This process significantly changes the Ta-d component of the electronic local density of states (Fig. 2).

Within the same transition metal atom, TaC and TaN compounds are characterized by a common LDOS pattern (Fig. 2) of the bonding and anti-bonding states. Yet, the position of the Fermi level, which determines the occupation of those states, changes from 1.24 eV in TaC to 1.34 eV in TaN, which is also fixed by the number of valence electrons per Ta–C(N) pair. The Chemical bonding in tantalum carbide and nitride is a complex interplay of covalent, metallic, and ionic components. All three types of bonding mainly involve Ta-d and C(N)-2p atomic orbitals.

4. Conclusion

In this paper, we present a complete analysis of structural, elastic and electronic properties of tantalum compounds, i.e. TaC and TaN, using the FP-LAPWl + *lo* method. The use of the LDA and GGA for the exchange-correlation potential permitted us to obtain good structural parameters. We compare our band structure to those calculated by Papaconstantopoulos [37], Gupta and Freeman [44], and a good agreement is found. We are not aware of any published data for elastic constants of TaN so our calculation can be used to cover this lack of data.

Acknowledgments

This work was supported by the Swiss National Science Fondation (NSF) and by the Swiss Federal Office of Education and Science (OFES) trough COST Action D26.

References

[1] J.R. Roos, J.P. Celis, E. Vancoille, H. Veltrop, S. Boelens, F. Jungblut, J. Ebberink, H. Homberg, Thin Solid Films 193–194 (1990) 547.
[2] J.S. Kim, J.W. Park, Bull. Korean Inst. Met. 1 (2) (1988) 144.
[3] L.E. Toth, Transition Metal Carbides and Nitrides, Academic, New York, 1971.
[4] E.K. Storms, The Refractory Carbides, Academic, New York, 1967.
[5] K. Schwarz, J. Phys. C 10 (1977) 195.
[6] K. Schwarz, Solid State Mater. Sci. 13 (3) (1987) 211.
[7] P. Blaha, K. Schwarz, Int. J. Quant. Chem. XXIII (1983) 1535.
[8] J.F. Smith, O.N. Carlson, R.R. DeAvillez, J. Nucl. Mater. 148 (1987) 1.
[9] K. Frisk, G.A. Ferràndez, J. Alloys Comp. 238 (1996) 167.
[10] H. Wiesenberger, W. Lengauer, P. Ettmayer, Acta Mater. 46 (1998) 651.
[11] Tantalum, Landolt-Börnstein New Series IV/5H, Springer Verlag, Berlin, 1993, p. 231.
[12] T. Oyama (Ed.), The Chemistry of Transition Metal Carbides and Nitrides, Blackie Academic & Professional, London, 1996.
[13] A. Kaloyeros, X. Chen, T. Stark, K. Kumar, S.-C. Seo, G. Peterson, H. Frisch, B. Arkles, J. Sullivan, J. Electrochem. Soc. 146 (1999) 170.
[14] K.H. Min, K.C. Chun, K.B. Kim, J. Vac. Sci. Technol. B 14 (5) (1996) 3263.
[15] R. Rosenberg, D.C. Edelstein, C. Hu, K.P. Rodbell, Annu. Rev. Mater. Sci. 30 (2000) 229.
[16] D. Edelstein, J. Heidenreich, R. Goldblatt, W. Cote, C. Uzoh, N. Lusting, P. Roper, T. McDevitt, W. Motsiff, A. Simon, J. Dukovic, R. Wachnik, H. Rathore, R. Schulz, L. Su, S. Luce, J. Slattery, in: Technical Digest—International Electron Devices Meeting, 1997, p. 773.
[17] M.T. Wang, Y.C. Lin, M.C. Chen, J. Electrochem. Soc. 145 (1998) 2538.
[18] C. Angelkort, A. Berendes, H. Lewalter, W. Bock, B.O. Kolbesen, Thin Solid Films 437 (2003) 108.
[19] J.O. Olowolafe, C.J. Mogab, R.B. Gregory, M. Kottke, J. Appl. Phys. 72 (1992) 4099.
[20] T. Oku, E. Kawakami, M. Uekubo, K. Takahiro, S. Yamaguchi, M. Murakami, Appl. Surf. Sci. 99 (1996) 265.
[21] M.H. Tsai, S.C. Sun, C.E. Tsai, S.H. Shuang, H.T. Chiu, J. Appl. Phys. 79 (1996) 6932.
[22] M. Stavrev, D. Fischer, F. Praessler, C. Wenzel, K. Drescher, J. Vac. Sci. Technol. A 17 (1999) 993.
[23] P. Blaha, K. Schwarz, G.K.H. Madsen, D. Kvasnicka, J. Luitz, An augmented plane wave plus local orbitals program for calculating crystal properties, Vienna University of Technology, Austria, 2001, 3-9501031-1-2.
[24] K. Schwarz, J. Solid State Chem. 176 (2003) 319.
[25] K. Schwarz, P. Blaha, Comput. Mater. Sci. 28 (2003) 259.
[26] J.P. Perdew, K. Burke, M. Ernzerhof, Phys. Rev. Lett. 77 (1996) 3865.

[27] D.M. Ceperley, B.J. Alder, Phys. Rev. Lett. 45 (1980) 566.
[28] F.D. Murnaghan, Proc. Natl. Acad. Sci. USA 30 (1944) 244.
[29] M.J. Mehl, Phys. Rev. B 47 (1993) 2493.
[30] K. Kobayashi, Surf. Sci. 493 (2001) 665.
[31] Landolt-Bernstein, Numerical Data and Functional Relationships in Science and Technolgy, New Series, Group III: Crystal and Solid State Physics, vol. 17, subvolume g, Springer, Berlin, 1984.
[32] E.Z. Kurmaev, A. Moewes, Z.V. Pchelkina, I.A. Nekrasov, A.A. Rempel, D.L. Ederer, Phys. Rev. B 64 (2001) 073108.
[33] D.A. Papaconstantopoulos, Phys. Rev. B 31 (2) (1985) 752.
[34] H.B. Nie, S.Y. Xu, S.J. Wang, L.P. You, Z. Yang, C.K. Ong, J. Li, T.Y.F. Liew, Appl. Phys. A 73 (2001) 229.
[35] S.P. Dodd, M. Cankurtaran, B. James, J. Mater. Sci. 38 (2003) 1107.
[36] W. Weber, Phys. Rev. B 8 (1973) 5082.
[37] D.A. Papaconstantopoulos, W.E. Pickett, B.M. Klein, L.L. Boyer, Phys. Rev. B 31 (1985) 752.
[38] B.M. Klein, D.A. Papaconstantopoulos, Phys. Rev. B 32 (1974) 1193.
[39] D.A. Papaconstantopoulos, in: P. Rhodes (Ed.), Physics of Transition Metals 1980, IOP, London, 1981, p. 563.
[40] B.M. Klein, D.A. Papaconstantopoulos, L.L. Boyer, Phys. Rev. B 22 (1980) 1946.
[41] W.E. Pickett, B.M. Klein, D.A. Papaconstantopoulos, Physica 107B (1981) 667;
D.A. Papaconstantopoulos, W.E. Pickett, B.M. Klein, L.L. Boyer, Nature (London) 308 (1984) 494.
[42] K. Schwarz, H. Ripplinger, A. Neckel, Z. Phys. B 48 (1982) 79.
[43] P. Weinberger, R. Podloucky, C.P. Mallett, A. Neckel, J. Phys. C 12 (1979) 801.
[44] M. Gupta, A.J. Freeman, Phys. Lett. 57A (1976) 291;
Phys. Rev. Lett. 37 (1976) 364;
Phys. Rev. B 14 (1976) 5205.
[45] M. Ihara, M. Hirabayashi, H. Nakagawa, Phys. Rev. B 14 (1976) 1707.
[46] D.A. Papaconstantopoulos, L.L. Boyer, B.M. Klein, A.R. Williams, V.L. Moruzzi, J.F. Janak, Phys. Rev. B 15 (1977) 4221.
[47] K. Schwarz, CRC Crit. Rev. Solid State Mater. Sci. 13 (1987) 211.
[48] P. Blaha, J. Redinger, K. Schwarz, Phys. Rev. B 31 (1985) 2316.
[49] W.S. Williams, Mater. Sci. Eng. A 105/106 (1988) 1.
[50] L. Ramqvist, K. Hamrin, G. Johansson, A. Fahlman, C. Nording, J. Phys. Chem. Solids 30 (1969) 1835.
[51] J. Häglung, A.F. Guillermet, G. Grimvall, M. Körling, Phys. Rev. B 48 (1993) 11685.